JCF

*Journal of Complex Flow, Vol. 6 No. 1 (2024) p. 16-22*

**Journal of Complex Flow**

*Journal homepage: www.fazpublishing.com/jcf*

**e-ISSN : 2672-7374**


# Aerodynamic Study of High-Speed Train's Drag Coefficient by Computational Fluid Dynamics

**Muhammad Syafiq Shaiful Anuar[1], Azwan Sapit[1,*], Saad Kariem Shater[2]**

[1] Faculty of Mechanical and Manufacturing Engineering,
Universiti Tun Hussein Onn Malaysia, Batu Pahat, 86400, MALAYSIA
[2] Department of Production Engineering and Metallurgy,
University of Technology, Baghdad, IRAQ

*Corresponding Author

Received 15 Nov 2023;
Accepted 26 Dec 2023;
Available online 15 April 2024

**Abstract:** This research focuses on studying airflow characteristics on three selected models of high-speed trains' body surfaces with different velocities. There will be nine simulation case results consisting of the data about drag coefficient, drag force, lift force, and lift coefficient. This study focuses on the drag coefficient by using the Computational Fluid Dynamics. Three high-speed train models have been designed, which are modelled from Tokaido Shinkansen N700s (Japan), Shanghai Maglev (China) and KTX-Eum (South Korea). With a lack of data and less information about the High-Speed Trains model due to the private and confidentiality of each company, only a simple design had been made but still looked the same as the real-life high-speed trains model with real scale value. For the velocity, Tokaido Shinkansen N700s were set to 79.1667 m/s, 50 m/s and 25 m/s, while Shanghai Maglev were set to 119.72 m/s, 69.305 m/s and 41.66 m/s. For the KTX-Eum, the velocity was set to 79.44 m/s, 50 m/s and 25 m/s. The result shows the different trend of coefficient between the three High-Speed Trains models. The data has been collected, and the lowest value for ecoefficiency was Tokaido Shinkansen N700s (Japan). It's proof that the lowest value of each coefficient will be used to determine which model has great aerodynamic efficiency performance with the speed gain but low usage of energy such as electricity. The higher the speed or velocity, the higher the velocity streamlines, thus creating a powerful downward airflow that can generate higher thrust force.

**Keywords:** CFD, Airflow, Drag Coefficient, High-Speed Trains, Aerodynamic

## 1. Introduction

The lateral aerodynamic performance of high-speed trains has drawn much attention due to increased speed. As train speed and crosswind velocity increase, the operating safety of high-speed trains under crosswind situations drastically declines. A high-speed moving at 200 km/h risks derailing or overturning when the crosswind speed exceeds 30 m/s. Using numerical models and actual data, Baker et al. evaluated high-speed trains' flow structure and aerodynamic properties in crosswinds [1]. Suzuki et al. use wind tunnels to test the aerodynamic properties of stationary trains across bridges and embankments [2]. Using experimental techniques and computer models, Diedrich et al. [3] investigated the flow structure of a high-speed train moving up a 6m high embankment.

According to the estimated and actual statistics, the train travelling on an embankment's leeward side had worse aerodynamic performance than the train travelling on its windward side [4-6]. A high-speed train operating in crosswinds on various infrastructures, including tracks, embankments, and viaducts, was studied by Zhang et al. for its unstable aerodynamic features and operational safety. According to the findings, trains operating on the leeward side of an embankment had inferior aerodynamic performance and were less safe to operate [7,8]. A train's head shape, which significantly impacts the aerodynamic properties of high-speed trains, can be altered to increase aerodynamic performance. Drawing up several high-speed train head designs, comparing them, and selecting the optimum head design based on wind tunnel testing results or computer simulations is frequent [9-11].

**Corresponding author: azwans@uthm.edu.my*

This approach is labour-intensive and significantly dependent on the designers' engineering expertise. A direct optimisation design technique has recently been used to optimise the head designs of high-speed trains, thanks to advancements in computer technology and optimisation algorithms [12,13]. Direct optimisation design uses mathematical techniquesto find the least or greatest of a few design goals while attempting to meet several constraints. Lee and Kim optimised the shape of the train's nose using a Kriging surrogate model to reduce the maximum micropores-sure wave generated by a high-speed train as it goes through a tunnel [14]. Krajnovic employed reaction surface techniques to create a high-speed train head to reduce aerodynamic drag and improve train stability in crosswinds. By integrating evolutionary algorithms and arbitrary shape deformation techniques, Sun et al. improved the head shape of China Railways High-speed 3 [15.

Yu et al. [16] developed a high-speed train head to decrease aerodynamic drag and the load reduction factor by combining several processes into multi-objective optimisation approaches. By integrating evolutionary algorithms with Kriging models, Yao et al. could optimise the head form of the high-speed train successfully. Mun oz- Paniagua et al. [17] employed evolutionary algorithms and the aerodynamic drag force as the optimisation objectives to create a high-speed train head with the greatest feasible micro-pressure wave generated by the train travelling through a tunnel [18]. To accomplish a multi-objective optimisation of a high-speed train head in an open area with no crosswind, Li et al. employed evolutionary algorithms based on a Kriging model [19]

The sources frequently emphasise crosswind-free circumstances when discussing improvements to the head shapes of high-speed trains operating in the open. The instance of a train travelling on the leeward side of an embankment is the most crucial since it is well-known that a train performs worse aerodynamically in crosswinds than it does in circumstances without a crosswind [20-22]. The total aerodynamic drag coefficient, $C_d$, lift coefficient, $C_l$, and side coefficient, $C_s$ of the head coach were used in this study as the optimisation objectives to establish the multi-objective optimisation design process of the head shape of a high-speed train operating on the leeward side of an embankment in the crosswind conditions [23].

## 2. Design and Methodology

Three models of High-Speed Trains (HST) body surfaces with different velocities in each model will be simulated. There will be nine simulation case results consistent with the data about drag coefficient, drag force, lift force, and lift coefficient. Table 1 shows the initial condition involved in the simulation of each HST model.

**Table 1 – Physical and thermal properties of the base fluid**

| Cases | Tokaido Shinkansen N700S | Shanghai Maglev | KTX-Eum |
|---|---|---|---|
| Vel. 1, | 79.16 m/s | 119.72 m/s | 79.44 m/s |
| Vel. 2, | 50 m/s | 69.305 m/s | 50 m/s |
| Vel. 3, | 25 m/s | 41.66 m/s | 25 m/s |
| Air Temp. $T$ | 288.16 K (15°C) | | |
| Pressure, $P$ | 1 atm | | |
| Density, $\rho$ | 1.225 kg/m$^3$ | | |
| Dynamic viscosity, $\mu$ | $1.802 \times 10{-}5$ kg/ms | | |
| Kinematic viscosity, $v$ | $1.470 \times 10{-}5$ m$^2$/s | | |

Tokaido Shinkansen N700S

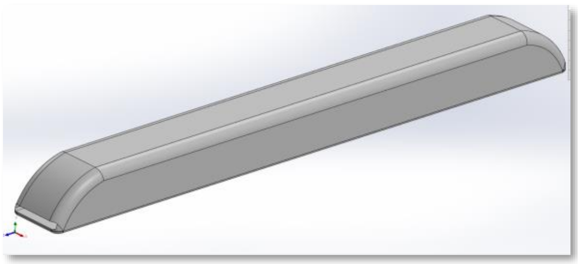

Shanghai Maglev

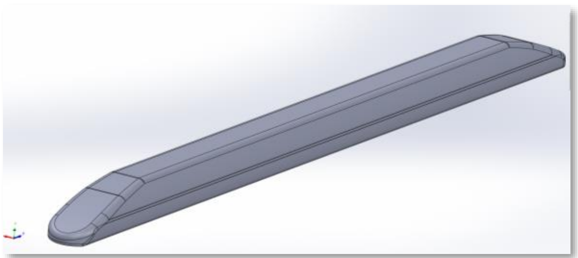

KTX-Eum

**Fig. 1 – Design for each HST**

### 2.1 Simulation Setup

The simulation and calculation use ANSYS Fluent software. Typically, engineering simulation begins with a drawing using Solidworks software. Once completed, the geometry files are transferred to the ANSYS software and saved in the STEP AP214 file format. Then, import the simulation into one of the ANSYS-provided software packages that is fluent and suited for fluid or air movement. Figure 2 shows the flow for ANSYS setup for simulation work, starting from geometry, meshing, setup and results analysis.


Published by FAZ Publishing
*http://www.fazpublishing.com/jcf*

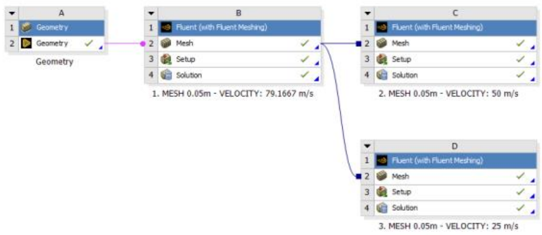


**Fig. 2 – The fluid flow (fluent) ANSYS software**

A wind tunnel analysis followed this study. The tunnel was designed so that the wind blows in just one direction. The wind tunnel method forces air around the target, giving the impression that it is moving. Strong blow air through the inlet High-Speed Trains body is utilised, and the object is securely fixed to prevent movement. The enclosure surrounding the High-Speed Trains model is set as the refinement domain, and the enclosure outer is the static domain. Figure 3 was a domain for the High-Speed Trains simulation using Ansys Software.

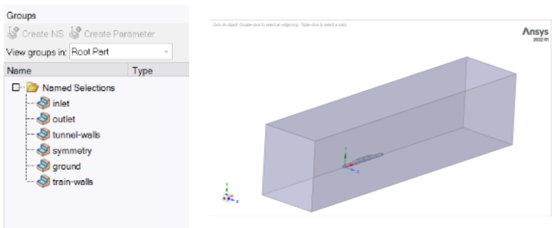


**Fig. 3 – Enclosure and name surface selection.**

## 2.2 Meshing and Parameter Setup

Before the numerical simulation, the High-Speed Trains and their entity and the computational domain must be defined. The mesh quality is critical since it directly affects the calculation accuracy and computational convergence speed [24,25]. Below are details of the mesh and the named selection for the face of the enclosure. Because of the largest scale used for this simulation, the refinement region parameter has been used for all three designs.

A watertight geometry workflow is utilised for this study. Hence, after carefully definingthe final volume of the geometry, the following step is to import the geometry into Fluent Meshing to mesh it. The fluid domain is separated into relatively small controlvolumes, known as cells, during the meshing process. The grid should have a minimum grid quality as indicated by orthogonality measures. A minimum skewness of 0.9 is sought in this simulation. Accordingly, to ensure that both the geometrical characteristics are adequately captured while minimising the computational load, the global parameters for all local sizing are set at a growth rate of 1.2, a minimum cell size of 0.05 m, and a maximum of 1.2 m. All size functions are assigned based on curvature and proximity by the default value of curvature normal angle at 18°. Additionally, after many trials of sizing combinations, a local refinement region is introduced, as shown in Table 2.

**Table 2 – Local refinement region parameter for all designs.**

| Mesh sizes | 0.05 m | | | |
|---|---|---|---|---|
| Domain parameter | $X_{min}$ | 0.3 m | $X_{max}$ | 0.3 m |
| | $X_{min}$ | 0.3 m | $X_{max}$ | 0.4 m |
| | $X_{min}$ | 0.3 m | $X_{max}$ | 0.6 m |

Figures 4 to 6 show the meshing for the simulation model, starting with the local refinement region parameter, clustered prism surface mesh generated and closed view prism surface mesh generated. For clustered prism surface and closed view, the figure was for Tokaido Shinkansen, as an example meshing for the simulation.

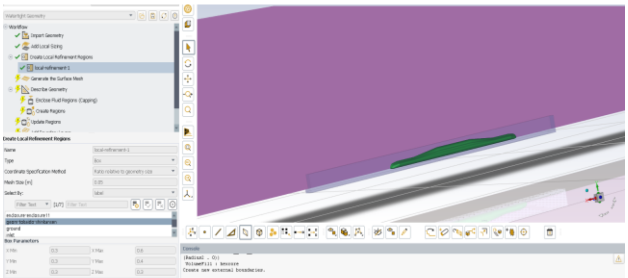

**Fig. 4 – Local refinement region parameter**

**Fig. 5 – Clustered prism surface mesh generated**

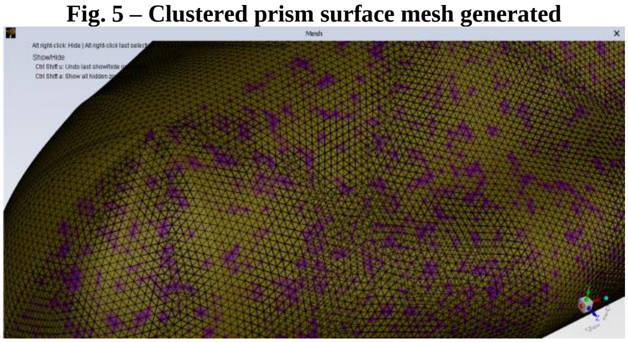

**Fig. 6 – Closed view prism surface mesh**

The size nodes and elements used are shown in the table below. The sizing element can be adjusted to set the size of nodes and elements. The smaller the size element of meshing, the more detailed the mesh. Besides, the meshing skewness is less than 0.9, so the result is still acceptable. This meshing progress uses 0.05 m size elements; improved volume meshing will use poly-hexacore type for finalisation. Table 3 summarises the mesh quality for all three cases.

**Table 3 – Mesh quality for simulation case with mesh 0.05 m**

| Cases | Number of Cells | No. of Nodes | Skewness |
|---|---|---|---|
| Tokaido Shinkansen | 14403037 | 20161845 | 0.10002843 |
| KTX-Eum | 9970624 | 15970436 | 0.10000012 |
| Shanghai Maglev | 8753184 | 12761392 | 0.10009764 |


Published by FAZ Publishing
*http://www.fazpublishing.com/jcf*

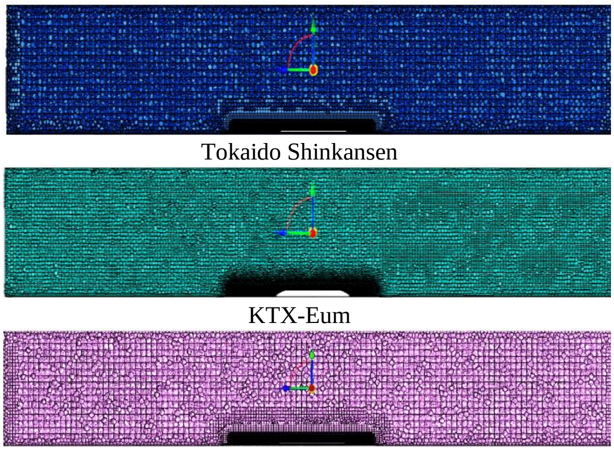


**Fig. 7 – Overall poly-hexacore volume mesh with refinement**

## 2.3 Simulation Setup

In this research paper, each model has been used to analyse that has a different velocity value towards the airflow movement through the High-Speed Train model surface from the nose head to the rear part. The parameters for the simulation setting are summarised in Table 4.

**Table 4 – Parameter for simulation setup**

| Parameters | Values | | |
|---|---|---|---|
| HST model | **Tokaido Shinkansen** | **Shanghai Maglev** | **KTX-Eum** |
| Area, $m^2$ | **6.1591** | **3.9133** | **4.1378** |
| Velocity, $V$ *(m/s)* | **79.16** | **119.72** | **79.44** |
| Fluid density, $\rho$ | | **1.225 kg/m³** | |
| Turbulent length scale, $l$ | | 1 m | |
| Turbulent intensity, $I$ | | 0.5% | |
| Temperature, $K$ | | 288.16 | |
| Angular velocity, $\omega$ | | 185.2 rad/s | |
| Reynolds number, $Re$ | | $18\times10^6$ | |

## 3. Results and Discussion

This section will discuss the results obtained from the simulation work. It started with the verification of the meshing through the Grid Independent Test (GIT), followed by the results for the drag and lift coefficient for all models tested. Another interesting parameter discussed here is the pressure during each model's flow and the velocity streamlines.

## 3.1 Verification of Mesh with GIT

Regarding computational power, the finest mesh took approximately 14 hours to generate, whereas the medium and coarsest meshes took only 10 and 6 hours to complete the iterations. Among the three various meshes evaluated (20.16 million, 15.97 million, and 5.8 million cells with a single car geometry), the medium mesh is chosen for the study since the results for the drag coefficient did not differ substantially. The grid size is deemed acceptable since it is nearly identicalto the one used to compare the findings to the real results. Therefore, it is also preferable to select the medium mesh for the following study since computational costs do not entirely reflect a significant constraint. The acceptable degree of detail and definition that the mesh could give is more than compensated for the cost of processing time and consumption. The number of nodes, lift coefficient value, average time completion and skewness of those three varying mesh simulations are presented in Table 5.

**Table 5 – Meshing setup effect on the drag coefficient.**

| Configuration | Coarse | Medium | Fine |
|---|---|---|---|
| Total number of nodes | **5 825 652** | **15 970 436** | **20 161 845** |
| Drag coefficient | **1.0618** | **1.17623** | **1.2320** |
| Time to converge | **6** | **10** | **14** |

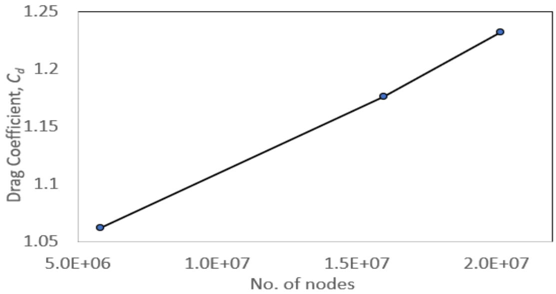


**Fig. 8 – Graph plot of mesh setup on drag coefficient**

## 3.2 Drag and Lift Coefficient

Figure 9 shows the graph velocity against $C_d$; the graph shows that the drag coefficient increases as the speed increases. Tokaido Shinkansen has the lowest $C_d$ compared to the Shanghai Maglev and KTX-Eum. In terms of energy use, the lower the coefficient, the lower the energy usage. In Figure 10, the graph shows the speed increase, the drag coefficient also increases, and Tokaido Shinkansen again has the lowest $C_l$ compared to the Shanghai Maglev and KTX-Eum.

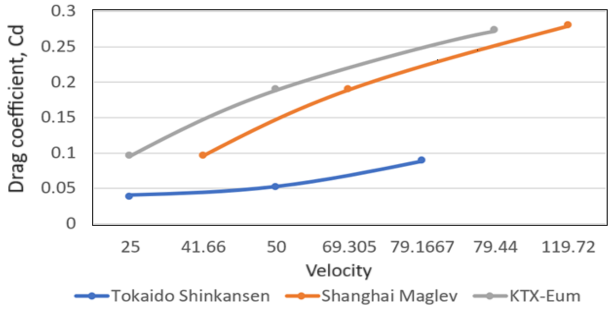


**Fig. 9 – Drag coefficient vs velocity for the models simulated**

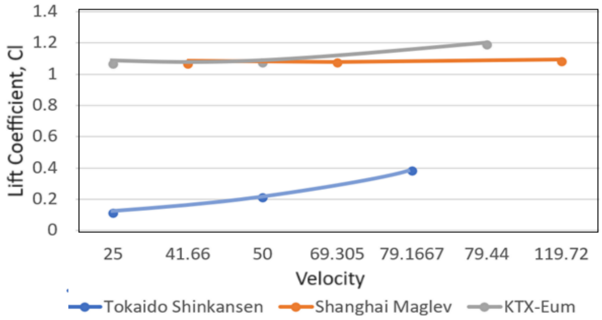


**Fig. 10 – Lift coefficient vs velocity for the models simulated**


Published by FAZ Publishing
*http://www.fazpublishing.com/jcf*

### 3.3 Pressure distribution

Figure 11 shows that the High-Speed Trains' head nose is red. This shows that the maximum pressure occurs at the head nose and decreases towards the back of High-Speed Trains. The pressure is lower at certain points on the surface of high-speed trains but high at the tip of the nose. As can be observed from the figure, at velocity 79.1667 m/s, the tip is 281 Pa, while at 50 m/s and 25 m/s, it is 111 Pa. As can be seen, the red colour becomes prominent at the head and nose as speed increases. The pressure at the nose head of the High-Speed Trains, especially around the Nose head, increases as the speed increases. The lift is produced when airflow across the body surface creates high and low-pressure zones. Quicker air flows over the top of the high-speed trains' body, resulting in low air pressure, while slower air goes beneath the high-speed trains, pushing forward.

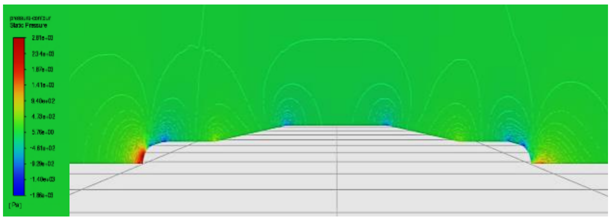

79.1667 m/s

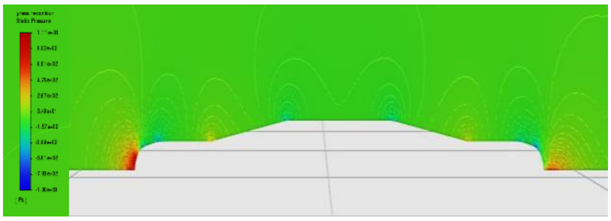

50 m/s

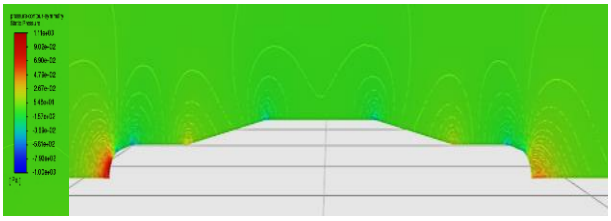

25 m/s

**Fig. 10 – Pressure contour for Tokaido Shinkansen**

From Figure 11, pressure at the Shanghai Maglev head nose increases as speed, especially at the nose head. At a velocity of 119.72 m/s, the pressure at the nose head is 697 Pa, and the lowest pressure is at the back of high-speed trains. The pressure is different between the back and nose heads of high-speed trains. The dark blue colour on the High-Speed Trains body surface indicates the lowest pressure, which acts on the top surface around the edges and has a value of -921 Pa.

119.72 m/s

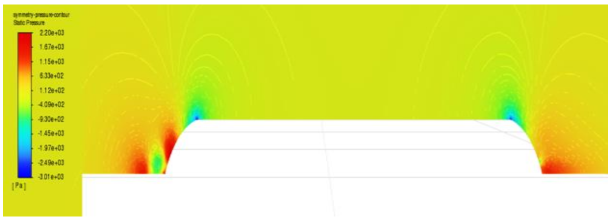

69.305 m/s

41.66 m/s

**Fig. 11 – Pressure contour for Shanghai Maglev**

From Figure 16, the increase in speed is the same as the effect of the increase in pressure. The top of the surface High-Speed Trains has the lowest pressure for the 3 velocities while high pressure at the nose head and back High-Speed Trains model. Only 25 m/s seems to have a large-scale dark blue region on the top of the surface edges. High-speed trains indicate the lowest pressure, which is -903 Pa. At 50 m/s, the blue region at the surface is still seen but not too large, like the velocity of 25 m/s. The greenish colour at the middle High-Speed Trains surface shows average airflow hit that area higher pressure around the nose head because of the body's movement. High-speed trains were fast, and the nose head was the main part that broke through the air while moving. The pressure near the upper surface of the High-Speed Trains is significantly lower than that near the lower surface (nose head). Most of the thrust the High-Speed train body generates is in the lowest part and nose head.

79.44 m/s

50 m/s

25 m/s

**Fig. 12 – Pressure contour for KTX-Eum**



Published by FAZ Publishing
*http://www.fazpublishing.com/jcf*

Furthermore, a negative pressure zone on top of the High-Speed Trains' edge surface indicates that the air flowing over the surface has just flown away from the High-Speed Trains edge surface. It is feasible to determine that the negative pressure generated on the edge surface of High-Speed Trains contributes more to lift creation than the high pressure generated on the bottom surface by comparing the measured pressure levels in this simulation.

### 3.4 Velocity Streamlines

Tokaido Shinkansen has been chosen for the reference result during the simulation work. In this case, three different velocities have been set. The velocities have been set at 79.1667 m/s, 50 m/s and 25 m/s. The simulation is made in Ansys Fluent software in 3-D form. The result of the velocity can be seen in Figure 13 below.

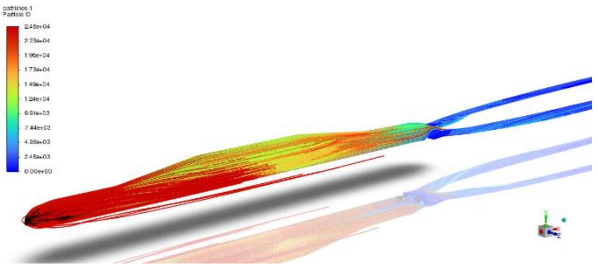

79.1667 m/s

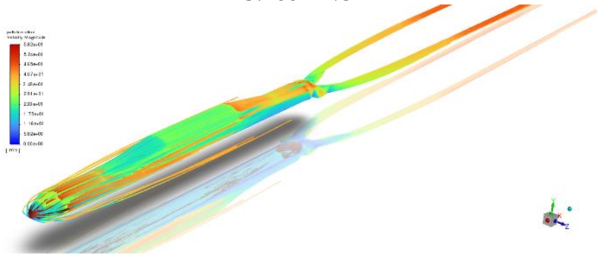

50 m/s

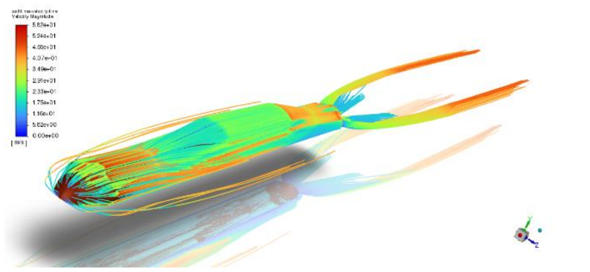

25 m/s

**Fig. 13 – Velocity streamline of the Tokaido Maglev**

Figure 13 shows the velocity streamlines while High-Speed Trains are moving continuously with the velocity that has been chosen. The air entering the inlet is drawn into the high-speed trains' body region, which moves with the body surface before exiting through the outlet. The airspeed increases as the velocity increases. At 25 m/s, the velocity streamline at the nose head is not as powerful as the velocity 50 m/s and 79.1667 m/s. The air becomes intense, especially at a velocity of 79.1667 m/s, and as shown above, the movement of air at the nose head becomes high pressure when the velocity is increased.

## 4. Conclusion

High-speed trains consist of an aerodynamic surface downforce generated in the movement of airflow with different velocities in each model. The lowest coefficient achieved was found to be that of the Japanese shinkansen; even their top velocity cannot challenge the Shanghai Maglev 119.72 m/s but still get the result lowest coefficient value, and it is proof that the surface design of nose head High-Speed Trains is the main thing about the aerodynamic effect for the air flow moving on their body surface and it's affected the performance. It's shown in more detail from the result between 3 designs of HST; Tokaido Shinkansen, Shanghai Maglev and KTX-Eum. For future work, it suggested simulating another model of high-speed trains to look at the capability of the Ansys Fluent to simulate the high-speed train. For instance, the first velocity may be 70 m/s, the second 50 m/s, and the last 25 m/s. This method was chosen because it will produce more accurate and comparable results to other designs. In addition, the approach used to view the airflow on the surface body of high-speed trains can be altered by sharpening the velocity contour.

**Acknowledgement**

The authors would like to express their gratitude to the Faculty of Mechanical and Manufacturing Engineering at Universiti Tun Hussein Onn Malaysia for supporting the completion of this research

**References**

[1] M. Mustafa. T. Hayat and S. Obadiat, "On heat and mass transfer in the unsteady squeezing flow between parallel plates." *Mechanica*, 47, 1581-1589, 2012.

[2] T. Hayat, et. al., "MHD squeezing flow of second grade fluid between two parallel disk", *International Journal of Numerical Fluids*, 69, 399-410, 2011.

[3] G. Domairry and A. Aziz. "Approx. analysis of MHD squeeze flow between two parallel disks with suction or injection by homotopy perturbation method", *Mathematical Problems in Engineering*.

[4] A. M. Siddiqui, S. Irum and A. R. Ansari. "Unsteady squeezing flow of a viscous MHD fluid between parallel plates." *Mathematical Modeling and Analysis*, 13, 565-576, 2008.

[5] A. M. Rashidi, H. Shahmohamadi and S. Dinarvand. "Analytic approximate solutions for unsteady two dimensional and axisymmetric squeezing flows between parallel plates." *Mathematical Problems in Engineering*, vol.2008,doi:10.1155/2008/935095.

[6] W. A. Khan and A. Aziz "Natural convective boundary layer flow over a vertical plate with uniform surface heat flux", *International Journal of Thermal Sciences*, 50, 1207-1217,2011.

[7] W. A. Khan W.A. and Aziz A. "Double diffusive natural convection boundary layer flow in a porous medium saturated with a nanofluid over a vertical plate, prescribed surface heat, solute and nanofluid fluxe." *International Journal of Thermal Sciences*, 50, 2154-2160,2011.

[8] A. J. Kuznetsov and N. D. Nield. "Natural convective boundary layer flow of a nanofluid past a vertical plate." *International Journal of Thermal Sciences*, 49, 243-247,2010.

[9] M. R. Hashimi., T. Hayat and A. Alsaedi. "On the analytic solutions for squeezing flow of nanofluids between parallel disks", *Nonlinear Analysis Modeling and Control*, 17(4), 418-430, 2014.

[10] C. L. M. H. Navier. "Memoir sur les lois du movement des fluids", *Memoirs Academic Royal Science Institute France*, 6, 389-440, 1823.

[11] C. H. Choi, J. A. Westin and K. S. Breur. "To slip or not slip water flows in hydrophilic and hydrophobic microchannels", Proceedings of IMECE 2002, New Orleans, LA, Article ID: 33707, 2002.

[12] M. T. Matthew and I. D. Boyd, "Nano boundary layer equation with nonlinear Navier boundary condition", *Journal of Mathematical Analysis and Application*, vol.333, pp.381-400, 2007.

[13] M. J. Martin and L. D. Boyd. Momentum and heat transfer in a laminar boundary layer with slip flow", *Journal of Thermo physics and Heat Transfer*, 20(4), 710-719, 2006.

[14] P. D. Ariel. Axisymmetric flow due to stretching sheet with partial slip", *Computer and Mathematics with Application*, 333, 381-400, 2007.

[15] C. Wang. Analysis of viscous flow due to a stretching sheet with surface slip and suction", *Nonlinear Analysis:Real world application*, 10(1), .375-380, 2009.

[16] K. Das. Impact of thermal radiation on MHD slip flow over a flat plate withvariable fluid properties", *Heat and mass transfer*, 48, 767-778, 2012.

[17] K. Das. Slip effects on heat and mass transfer in MHD micro polar fluid flow over an inclined plate with thermal radiation and chemical reaction", *International Journal of Numerical methods in Fluids*, 70, 96-101, 2016.

[18] A. Hussain, S. T. ,Mohyud-Cheema and T. A. Din. Analytical and numerical approaches to squeezing flow and heat transfer between two parallel disks with velocity slip and temperature jump", *China Physics Letter*, 29, 1-5,2012.

[19] K. Das. Slip flow and convective heat transfer of nanofluid over a permeable stretching surface", *Computers and Physics*, 64(1), 34-42, 2012.

[20] R.G. Deissler. An analysis of second-order slip flow and temperature-jump boundary conditions for rarefied gases. *International Journal of heat and mass transfer*. Vol. 7(6),681-694, 1964.

[21] K. Das., Jana S. and Acharya N., "Slip effects on squeezing flow of nanofluid between two parallel disks", International *Journal of Applied Mechanics and Engineering*, 21(1) , 5-20,2016.

[22] R.Ellahi. Hayat T., Mahomed F.M. and Asghar S. "Effects of slip on nonlinear flows of a third grade fluid", *Nonlinear Analysis: Real world Applications*, 11, 139-146, 2010.

[23] S. Yao T. Fang and Y. Zhang. "Heat transfer of a generalized stretching/shrinking wall problem with convective boundary condition", *Communications in Nonlinear science and Numerical simulation*, 16, 752-760, 2011.

[24] R. Kandasamy, P. Loganathanb and P. P. Arasub. "Scaling group transformationfor MHD boundary layer flow of a nanofluid past vertical stretching surface in the presence of suction/injection", *Nuclear Engineering and Design*, 241, 2053-2059,2011.

[25] D. Makinde and A. Aziz. "Boundary layer flow of a nanofluid past a stretching sheet with convective boundary conditions", *International Journal of Thermal sciences*, 50, 11326-1332, 2011.

[26] M. J. Uddin YasserAlginahiO. Anwar Bég·M.N.Kabir. "Numerical solutions for gyrotactic bioconvection in nanofluid-saturated porous media with Stefan blowing and multiple slip effects." *Computers & Mathematics with Applications*. Volume 72, Issue 10, November 2016, Pages 2562-2581

[27] M.J.Uddin M.N.Kabir Y.M.Alginahi. "Lie group analysis and numerical solution of magnetohydrodynamic free convective slip flow of micropolar fluid over a moving plate with heat transfer." *Computers & Mathematics with Applications*, Vol. 70, Issue 5, September 2015, Pages 846-856

*[28]* Md. Jashim, Uddin, W. A. Khan, and A. I. Md. Ismail· ¨Scaling Group Transformation for MHD Boundary Layer Slip Flow of a Nanofluid over a Convectively Heated Stretching Sheet with Heat Generation." *Mathematical Problems in Engineering.*


Published by FAZ Publishing
*http://www.fazpublishing.com/jcf*